

Asymmetric multi-component trifunctionalization reactions with α -Halo Rh-carbenes

Received: 7 September 2024

Accepted: 21 January 2025

Published online: 07 February 2025

Check for updates

Xiaoyan Yang^{1,3}, Xiaoyu Zhou^{2,3}, Wenhao Hu¹✉ & Yu Qian¹✉

Multi-component multi-functionalization reactions involving active intermediates are powerful tools for rapidly generating a wide array of compounds. Metal carbynoids, with their distinct reactivity, hold great promise for developing synthetic methodologies. However, their application in catalytic transfer reactions has been hindered by the limited availability of suitable precursors. In this study, we investigate the catalytic potential of α -halo Rh-carbenes, leveraging the concept of metal carbynoids in multi-functionalization reactions. Through a chiral phosphoric acid-catalyzed asymmetric trifunctionalization, we have developed a method for synthesizing a variety of chiral α -cyclic ketal β -amino esters with high yields and excellent enantioselectivity. Our extensive experimental and computational studies reveal that α -halo Rh-carbenes exhibit carbynoid properties, which facilitate the transformation into functionalized Fischer-type Rh-carbenes through the decomposition of the C-halo bond.

Multi-functionalization reactions^{1–6}, involving multiple components^{7–13} with active intermediates, are indispensable tools in both synthetic and medicinal chemistry. These reactions offer an efficient approach to constructing multiple chemical bonds in a single operational step by integrating three or more starting materials. They enable the rapid exploration of diverse chemical spaces and offer streamlined pathways to structurally varied compounds with a broad range of biological activities^{14–18}. Metal carbynoids^{19–23}, which exhibit dual reactivity as both carbene and carbon cation, can form up to three sigma bonds on a single carbon. This distinctive reactivity positions them as powerful intermediates, holding significant promise for advancing synthetic methodologies and facilitating the synthesis of complex molecules^{24–26}.

In recent years, the Suero group has reported a series of investigations utilizing hypervalent iodine Rh-carbenes as metal carbynoids. These investigations primarily focused on cycloaddition reactions with unsaturated olefins and acetylenes, leading to the formation of allyl structural units, cyclopropenes, and cyclopropyl-fused lactones^{27–29}. In 2023, our group pioneered asymmetric trifunctionalization reactions using the same reagents, successfully generating optically pure β -

amino esters³⁰. More recently, sulfonium Rh-carbenes have been utilized as metal carbynoids in two distinct applications: Han's group utilized them for synthesizing imidazo N-heterocycles through [2 + 1 + 2] cycloadditions³¹, while the Alcarazo group applied them in a ring expansion process to convert indenenes into naphthalenes³². Despite these advancements, the application of these active intermediates in catalytic transfer reactions remains largely unexplored. This is primarily due to the limited availability of suitable precursors^{33–35}. Overcoming this challenge could open alternative avenues for the development of efficient and innovative synthetic strategies.

α -Halo metal carbenes, developed by Bonge-Hanson's group^{36–42}, have demonstrated significant utility in a variety of metal-catalyzed reactions, including X-H insertion^{37,38}, cyclopropanation^{36,42} and as C1 synthons in carbon atom insertion reactions^{39,41} for skeletal editing^{43–45}. Despite these successes, their potential as precursors to metal carbynoids in catalytic processes, particularly in enantioselective transformations, remains largely unexplored. This is largely due to the challenge posed by the lower departure capability of the C-X bond

¹State Key Laboratory of Anti-Infective Drug Discovery and Development, Guangdong Provincial Key Laboratory of Chiral Molecule and Drug Discovery, School of Pharmaceutical Sciences, Sun Yat-sen University, Guangzhou, China. ²School of Pharmaceutical and Chemical Engineering, Taizhou University, Taizhou, China. ³These authors contributed equally: Xiaoyan Yang, Xiaoyu Zhou. ✉ e-mail: huwh9@mail.sysu.edu.cn; qianyu5@mail.sysu.edu.cn

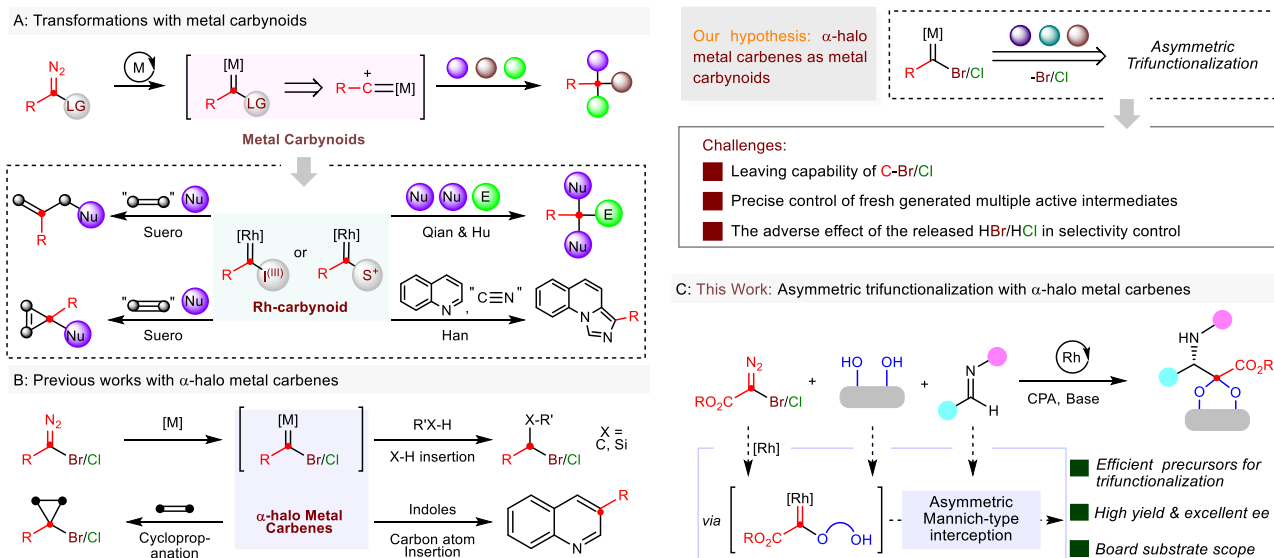


Fig. 1 | Transformations with metal carbynoids. A Transformations with metal carbynoids. **B** Previous works with α -halo metal carbenes. **C** Asymmetric trifunctionalization with α -halo metal carbenes (This work).

compared to C-^{III} / C-S⁺ bonds, as well as the need for precise control over the formation of multiple active intermediates. Additionally, the negative impact of liberated acids (such as HBr or HCl) on enantioselectivity, particularly within chiral acid control systems, presents a further obstacle that must be addressed to unlock their full potential.

Building upon our previous research on selective metal carbene multi-functionalization via ylide trapping process^{46–50}, we report here a chiral phosphoric acid-catalyzed asymmetric trifunctionalization reaction utilizing α -halo Rh-carbenes as carbynoids in combination with diols and imines (Fig. 1C). This method offers a rapid and efficient pathway to a diverse array of chiral α -cyclic ketal β -amino esters, which are of considerable interest due to their broad spectrum of biological activities^{51–54}, in high yields and exceptional enantioselectivities. The underlying mechanism has been thoroughly investigated through a combination of experimental and computational analyses.

Results

In our preliminary study, we evaluated a range of carbonyl precursors **1** with different types of leaving groups, including α -halodiazo esters, hypervalent iodine diazo reagents, and α -diazo sulfonium salts (Fig. 2). These reactions were conducted with diol **2a** and imine **3a** in CH₂Cl₂ at 0 °C in the presence of a Rh₂(OAc)₄ catalyst. We were pleased to observe that the reaction proceeded smoothly, with the bromo diazo ester **1a** providing the highest yield of 67%. Interestingly, the chloro diazo ester **11a** also afforded a satisfactory yield of 53%. Notably, the yield was further improved to 78% when 3.0 equivalents of **1a** were used. Subsequently, we assessed the performance of various commercially available transition metal catalysts to optimize the reaction conditions. Notably, both Rh₂(esp)₂ and Rh₂(Oct)₄ provided promising results, yielding the desired product in 69% and 67%, respectively. In contrast, Cu(MeCN)₄PF₆ and AgOTf, which are well-regarded for their efficacy in metal carbene transformations, were ineffective, failing to yield any desired product. Additionally, while [Pd(allyl)Cl]₂ did produce the desired product, the yield was significantly reduced to 32%. Encouraged by these preliminary results, we proceeded to explore enantiocontrol using phosphoric acid **4**. We were pleased to find that the expected chiral β -amino esters could be obtained in a 70% yield, albeit with <5% ee, utilizing 5.0 mol% of chiral phosphoric acid **4a**. Further investigation into various chiral phosphoric acids, ranging from **4b** to **4f**, revealed an improvement in enantioselectivity with the use of spiro-type chiral phosphoric acid **4d**, which resulted in an 84%

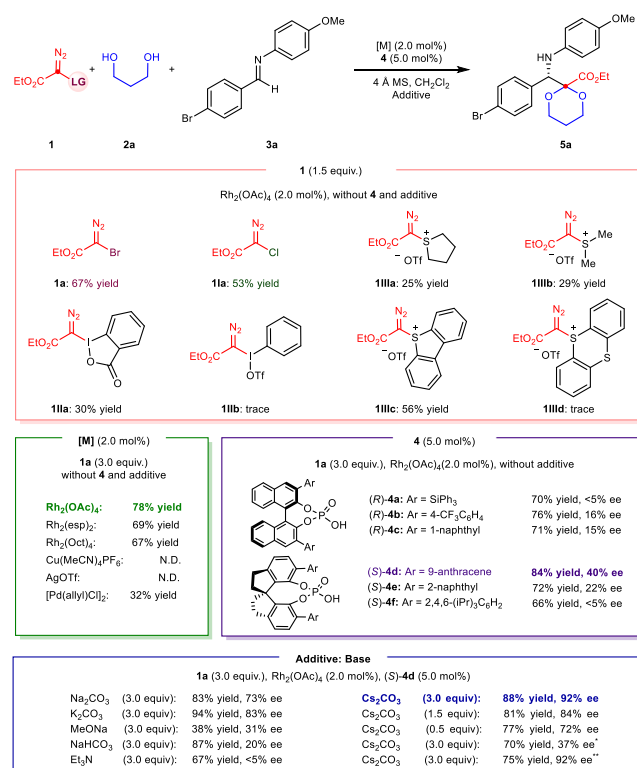


Fig. 2 | Reaction optimization. The reactions were conducted on a 0.1 mmol scale: To the mixture of corresponding catalyst (2.0 mol%), CPA **4** (5.0 mol%), **2a** (0.30 mmol), **3a** (0.10 mmol), and 4 Å MS (150 mg) in CH₂Cl₂ (1.5 mL) was added a solution of diazo compound **1** in cold CH₂Cl₂ (1.5 mL) by a syringe pump in 0.5 h under a nitrogen atmosphere at 0 °C; The yields were given as isolated yields, and the ee values were determined by chiral HPLC analysis; N.D. = not detected; *The reaction concentration was diluted to 0.011 mol/L; **15.0 mol% CPA (S)-**4d** was used.

yield and 40% ee for the desired product **5a**. Given the potential activation of the imine by HBr release during the reaction, which could impact the asymmetric control, we systematically explored different base additives. Gratifyingly, the addition of Cs₂CO₃ as an additive led to a significant enhancement in enantioselectivity control, leading to a

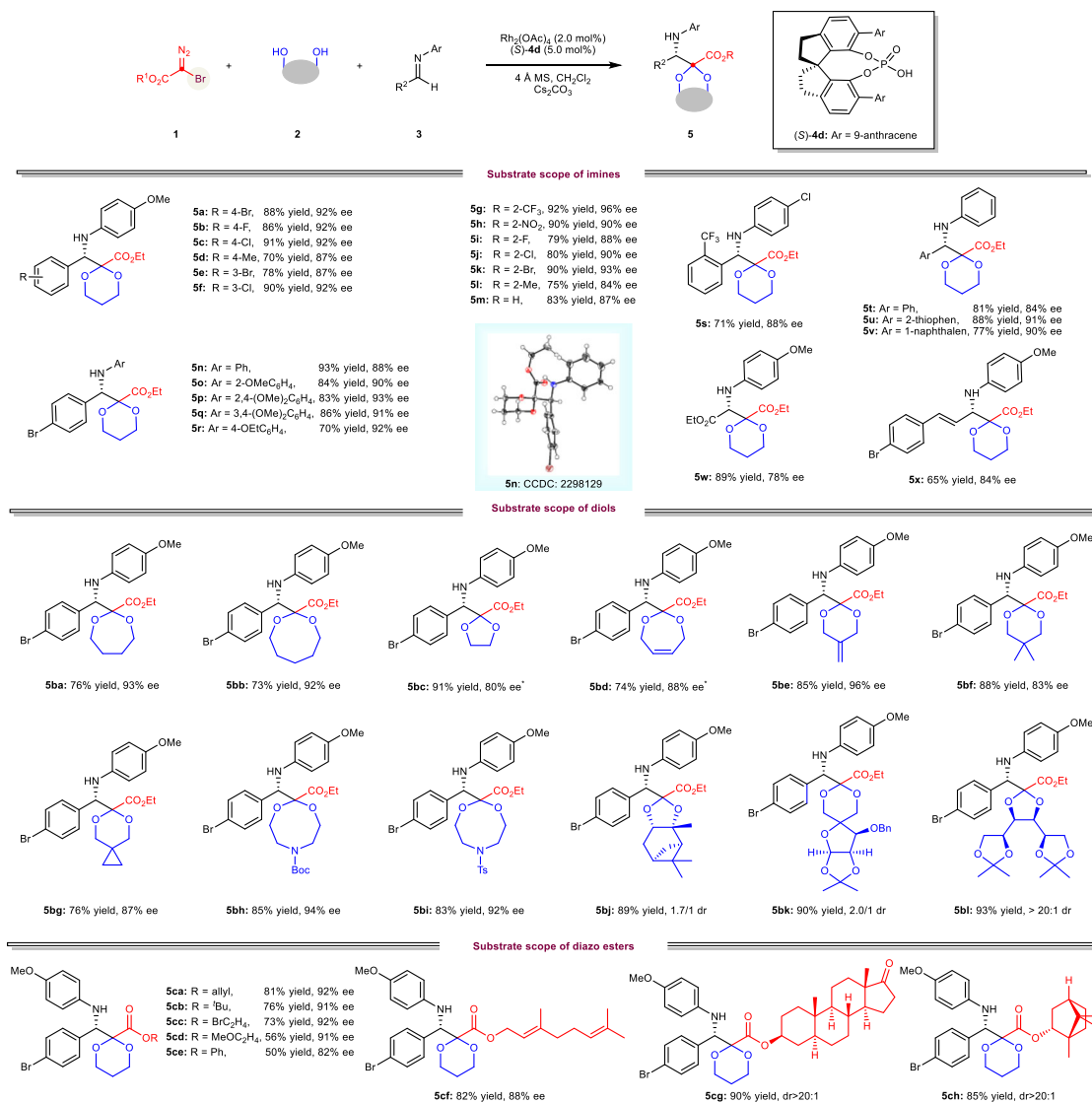


Fig. 3 | Substrate scope with α -bromo Rh-carbenes. The reactions were conducted on a 0.1 mmol scale: To the mixture of **3** (0.10 mmol), **2** (0.30 mmol), Rh₂(OAc)₄ (2.0 mol%), CPA **4 d** (3.3 mg, 5.0 mol%), Cs₂CO₃ (0.30 mmol) and 4 Å MS (150 mg) in CH₂Cl₂ (1.5 mL) was added a solution of diazo compound **1** (0.30 mmol)

in cold CH₂Cl₂ (1.5 mL) via a syringe pump in 0.5 h under a nitrogen atmosphere at 0 °C, and the reaction was running for 4 h under these conditions; The yields were given as isolated yields, the *dr* were determined by crude NMR and the *ee* values were determined by chiral HPLC analysis. *5.0 mol % Rh₂(OAc)₄ was used.

high 88% yield and excellent 92% *ee* for the desired product **5a**. Notably, reducing the amount of Cs₂CO₃ resulted in a lower isolated yield and enantiomeric excess, highlighting the importance of the base additive in controlling the selectivity of the reaction.

With optimized reaction conditions established, we expanded the applicability of the protocol to encompass various imines, diols, and diverse diazo esters (Fig. 3). Initially, we examined the substrate scope of imines **3** in conjunction with diazo compound **1a** and diol **2a**. Impressively, a wide array of functional groups on the aryl rings of the imines exhibited excellent tolerance, leading to the formation of Mannich-type addition products **5** with exceptional enantioselectivity and yields ranging from good to high. Specifically, imines **3** featuring benzaldehyde units at different positions, encompassing both electron-neutral and electron-withdrawing groups, yielded the desired products **5a-5m** in yields ranging from 70% to 92% with high 84-96% *ee*. Moreover, imines bearing various substituents on the aniline unit (Ar), such as hydrogen, halogen, and methoxy groups, demonstrated good reactivity, yielding products **5n-5t** with yields ranging from 70% to 93% and 84-93% *ee*. Smooth reactions were also observed for imines

derived from 2-thiophene and 1-naphthaldehyde, yielding products **5u** and **5v** in good yields and with high enantiomeric excesses of 90-91%. In addition to imines derived from aromatic aldehydes, those derived from cinnamaldehyde and ethyl glyoxalate emerged as practical reagents for this reaction, yielding the respective products **5w** and **5x** in good yields, albeit with slightly lower of 78-84% *ee*. The stereochemistry of **5n** was determined as *S* by single crystal X-ray diffraction analysis, while the stereochemistry of other compounds was tentatively assigned by analogy.

A diverse array of diols was subsequently examined under the optimized reaction conditions, leading to the smooth formation of the corresponding products. Diols with varying chain lengths exhibited robust performance, yielding β -amino esters bearing diverse cyclic ketal ring sizes **5ba-5bc** in yields ranging from 73% to 91% with high 80-93% *ee*. Furthermore, diols featuring alkene groups capable of undergoing cyclopropanation with carbene complex³⁷⁻⁴⁰ were also well tolerated, producing the target products **5bd-5be** in good yields of 74-85% with good 88-96% *ee*. Reactions involving substituted diols and diols containing nitrogen atoms proceeded efficiently, providing

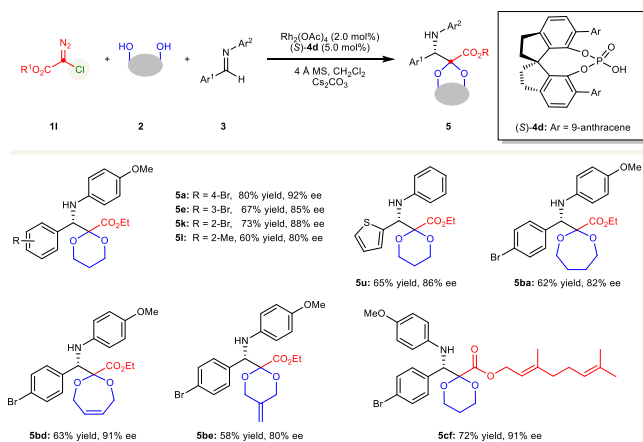


Fig. 4 | Substrate scope with α -chloro Rh-carbenes. Standard conditions as in Fig. 3.

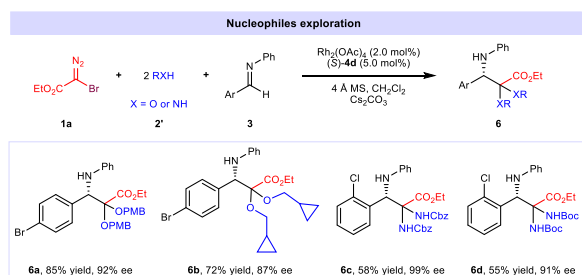


Fig. 5 | Synthetic generality. Expanding reactions with a range of nucleophiles.

products **5bf-5bi** in yields of 76–88% with remarkable enantiomeric excesses of 83–94%. Notably, naturally derived diols containing secondary and tertiary alcohols, such as Pinanediol, Ribofuranose and Mannitol, afforded the desired products **5bj-5bl** in high yields ranging from 89% to 93%. Finally, various ester groups of the diazo reagents were explored, all of which successfully provided the desired products **5ca-5ce** in good yields of 50–81% with 82–92% *ee*, even with bulky *t*Bu ester groups. Moreover, a range of naturally occurring alcohol-derived diazo reagents, including Geraniol, Epiandrosterone, and L(-)-Borneol were investigated, yielding their respective products **5cf-5ch** in high yields of 82–90% with excellent stereoselectivity (88% *ee* or >20:1 *dr*).

Next, we focused on establishing the catalytic asymmetric version of this transformation, utilizing chloro diazo esters as metal carbonynd precursors (Fig. 4). Under optimized conditions, a wide range of imines, featuring diverse electronic properties and substitution patterns, as well as diols, were evaluated. This led to the formation of the desired products **5** in 58–80% yield with high 80–92% *ee*. Alkene groups present in both diols and diazo esters were well-tolerated, yielding compounds **5bd** and **5cf** in good yields with enantiomeric excesses exceeding 91%. These findings demonstrate that chloro diazo esters can serve as effective carbonynd precursors in multicomponent reactions.

To further demonstrate the effectiveness of α -halo Rh-carbenes as metal carbonynds, we investigated the use of various nucleophiles (Fig. 5). Monoalcohols were well-tolerated under the standard reaction conditions, yielding the desired uncyclic β -amino esters **6a** and **6b** with good yields and excellent enantiomeric excesses of 92% and 87%, respectively. Additionally, carbamates with Cbz and Boc protecting groups also gave favorable results, resulting in the desired products **6c** and **6d** with excellent enantiomeric excesses of 99% and 91%, along with good yields.

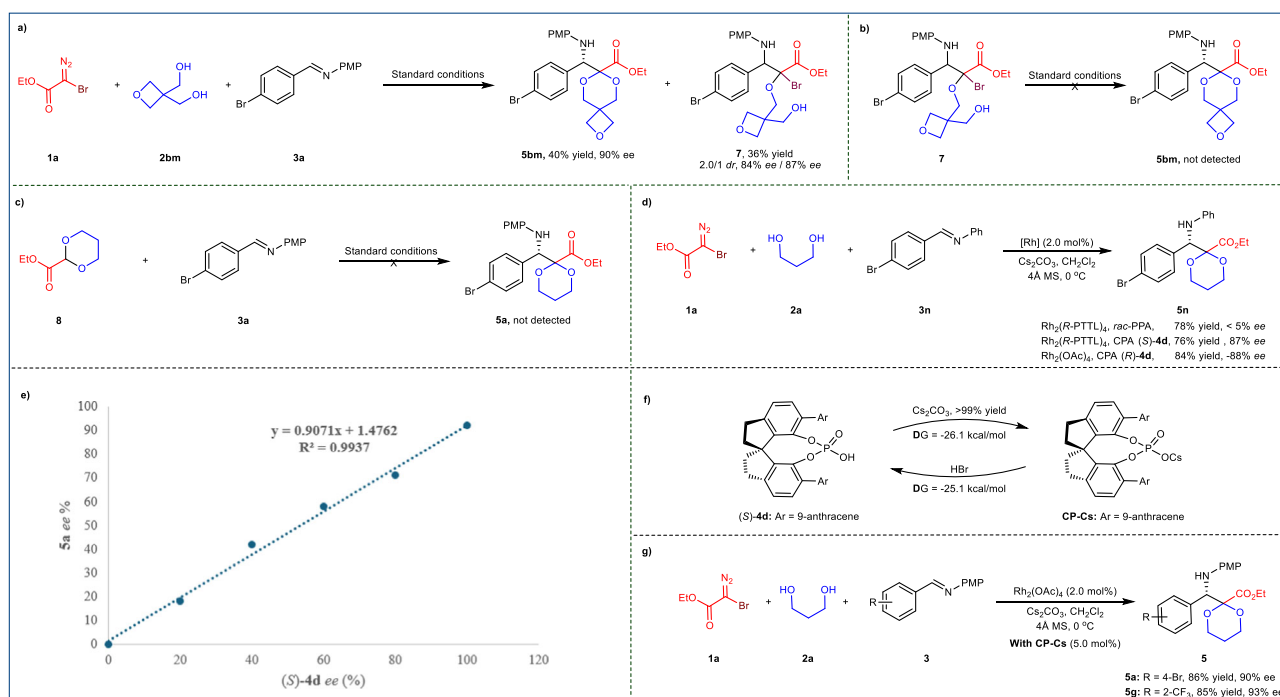


Fig. 6 | Control Experiments. **a** The reaction was performed with diol **2bm**. **b** Compound **7** was subjected to standard reaction conditions. **c** Compound **8** and imine **3a** were subjected to standard reaction conditions. **d** The reaction was

performed with chiral rhodium catalyst. **e** The study of nonlinear effect. **f** The synthesis of CP-Cs and the calculated gibbs free energy changes for CPA and CP-Cs. **g** The reaction was performed with CP-Cs as the chiral catalyst.

To gain insight into the mechanism underlying this trifunctionalization reaction, we conducted a series of control experiments. Using diol **2bm**, the desired product **5bm** was obtained in 40% yield with a high enantiomeric excess of 90%, while the typical ylide trapping product **7** was also detected in 36% yield (Fig. 6a). When isolated **7** was treated under standard conditions, no cycloaddition product **5bm** was observed (Fig. 6b), suggesting that the C-Br bond undergoes cleavage prior to the addition step. Next, we observed no reaction between the insertion product **8** and imine **3a** under standard reaction conditions (Fig. 6c), suggesting that a stepwise pathway is not likely. We then introduced $\text{Rh}_2(\text{R-PTTL})_4$ as the chiral catalyst along with racemic phosphoric acid, yielding the corresponding product **5n** in a high yield of 78%, but with enantioselectivity <5%. In contrast, using CPA (*S*)-**4d** led to a good yield of 76% with a high 87% *ee* (Fig. 6d). Similarly, when CPA (*R*)-**4d** was used as the chiral catalyst in combination with achiral $\text{Rh}_2(\text{OAc})_4$, the desired isomer was smoothly generated in a good yield of 84% with -88% *ee*. Furthermore, we observed a linear correlation between the enantiopurities of the products **5a** and their corresponding catalysts (*S*)-**4d**, indicating that a single chiral phosphoric acid (CPA) catalyst is involved in each enantioselective transition state (Fig. 6e). We also noted that CPA can react with Cs_2CO_3 under standard reaction conditions to form the cesium salt **CP-Cs**, with a calculated Gibbs free energy change (ΔG) of -26.1 kcal/mol. The **CP-Cs** salt can be acidified by HBr, converting it back to CPA, with a ΔG of -25.1 kcal/mol (Fig. 6f). When **CP-Cs** is employed as a chiral catalyst in trifunctionalization reactions in combination with

$\text{Rh}_2(\text{OAc})_4$, the desired products **5a** and **5g** can be obtained in high yields, achieving excellent 90% and 93% *ee*, respectively (Fig. 6g).

Subsequently, a density functional theory (DFT) using the quantum mechanics/molecular mechanics (QM/MM) methodology (two-layer ONIOM)⁵⁵⁻⁵⁷ was performed to elucidate the mechanism of Rh/CPA cooperatively catalyzed trifunctionalization with bromo diazo esters **1a**, as well as the origin of its stereoselectivity. As depicted in Fig. 7, the free energy profile for $\text{Rh}_2(\text{OAc})_4$ and CPA cooperatively catalyzed reaction starts from the carbynoid complex, **Cat-Rh**, through the reaction of **1a** with $\text{Rh}_2(\text{OAc})_4$, resulting in the extrusion of N_2 . The metal-alkyl intermediate **IM1** (-4.9 kcal/mol) is then formed following the addition of alcohol **2a** with metal-carbynoid via **TS1** (2.1 kcal/mol). The tautomeric isomer enol-intermediate **IM1-iso** is calculated to be energetically unfavorable, with an energy approximately 18.0 kcal/mol. From **IM1**, the reaction can proceed via two distinct pathways, labeled pathway A (red) and pathway B (blue). In pathway **A**, **IM1** undergoes dissociation of HBr to form the carbene **A-IM2** (-21.8 kcal/mol). With the assistance of another alcohol **2**, intramolecular nucleophilic addition from the **A-IM2** occurs through the transition state **TS2** (-10.8 kcal/mol) to form the intermediate **A-IM3** (-15.0 kcal/mol) or the enol-intermediate **A-IM3-iso** (-16.9 kcal/mol). Computational results show that the enol-intermediate **A-IM3-iso** is the favored species. Next, **A-IM3-iso** interacts with imine and CPA to form more stable interaction **A-IM4** (-41.0 kcal/mol), which is exergonic by 24.1 kcal/mol. The enantioselective *S*- and *R*- products are obtained via the transition state **A-TS3_S** (-42.5 kcal/mol) and **A-TS3_R** (-40.1 kcal/mol). The final product **5** is generated through ligand exchange

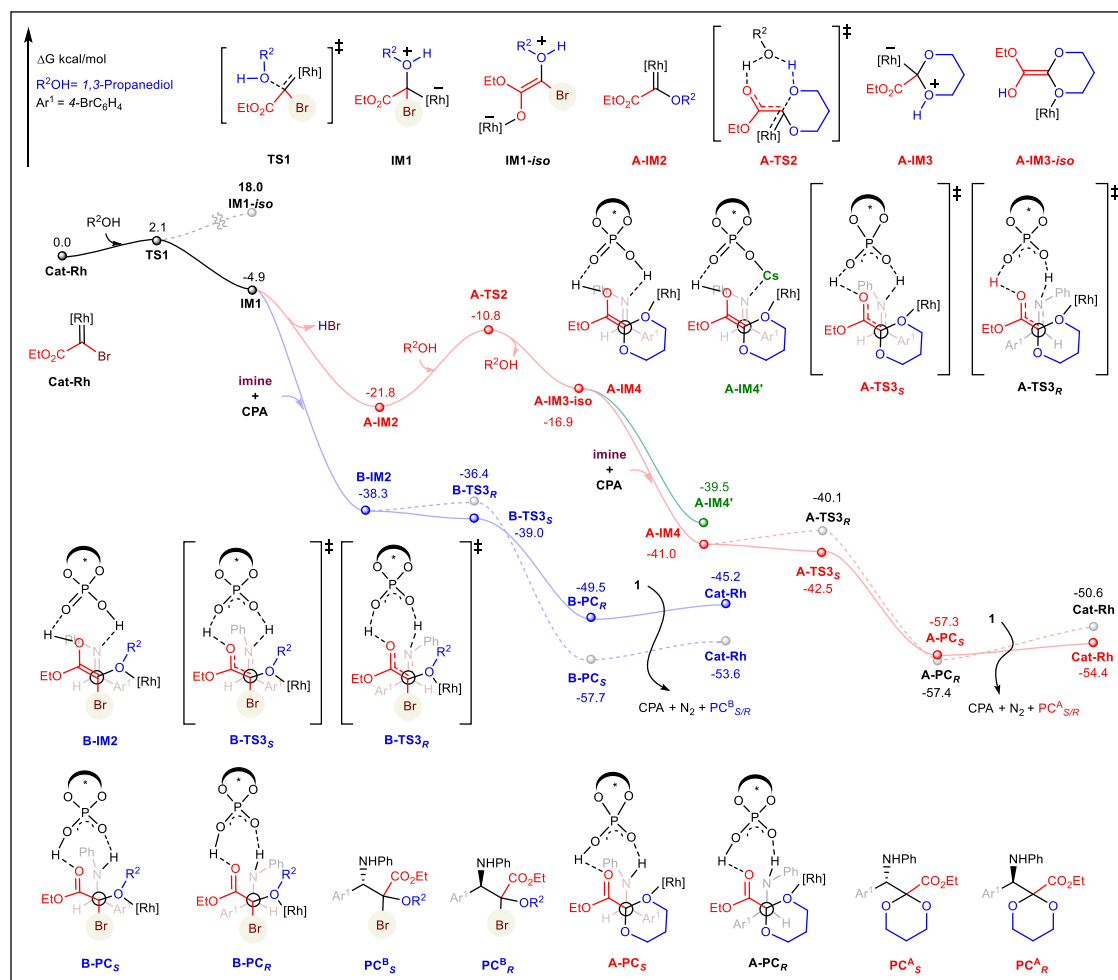


Fig. 7 | Free energy profile for the CPA catalyzed enantioselective trifunctionalization with α -bromo Rh-carbenes. Both the non-bromine products pathway (A, in red) and bromine products pathway (B, in blue) are explored. The former pathway was proved to be more favored.

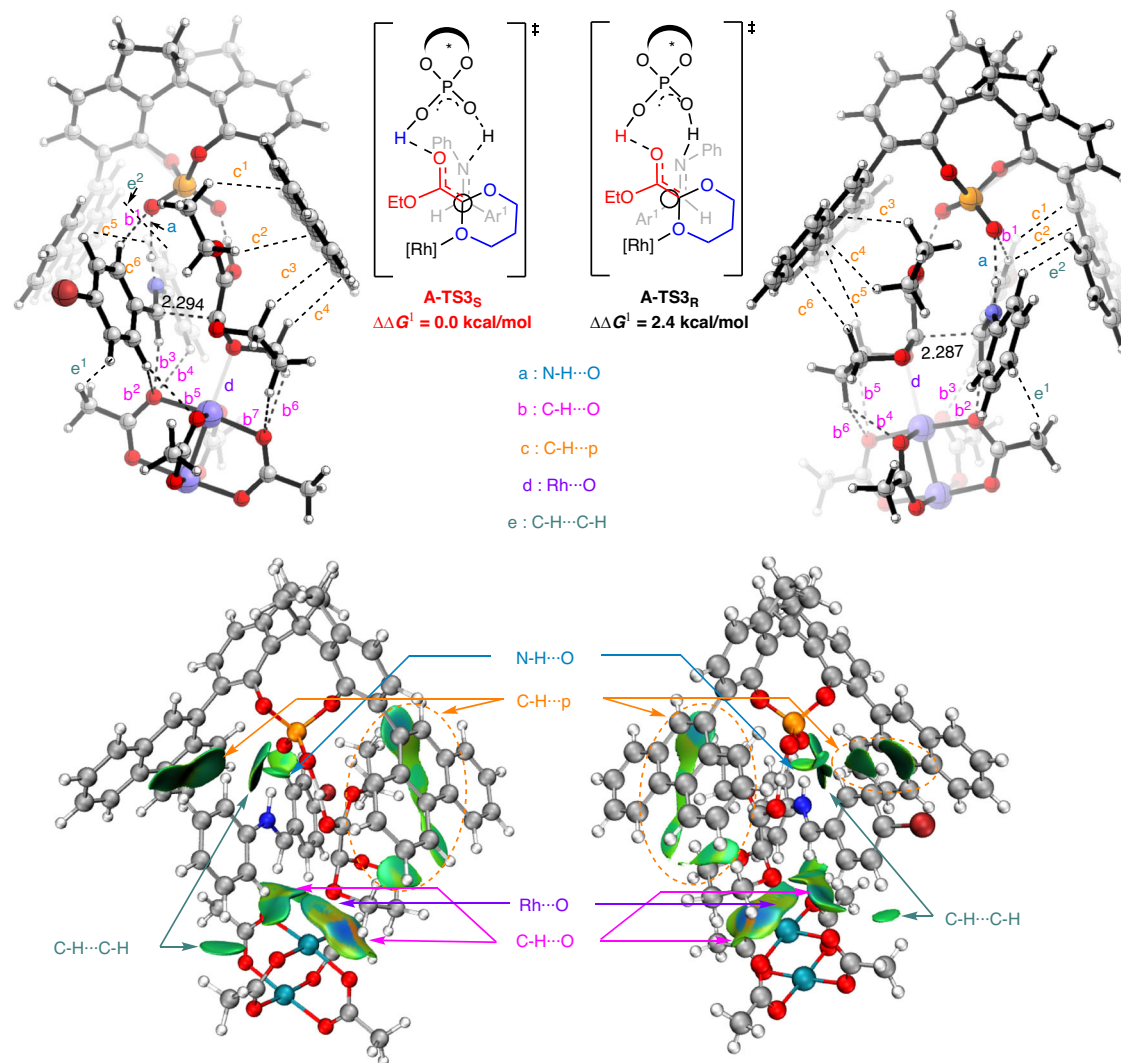


Fig. 8 | Key transition states and IGMH analysis of the non-covalent interactions for the $A-TS3_S$ and $A-TS3_R$. Noncovalent interactions play a pivotal role in the enantioselectivity control.

between the **A-PC** and the substrate **1a**, regenerating the carbynoid complex **Cat-Rh**. This entire process is exergonic by 54.4 kcal/mol. Alternatively, in pathway B, the ylide **IM1** directly interacts with imine and CPA to form intermediate **B-IM2** (-38.3 kcal/mol). Bromine-containing product in *S*- and *R*- configuration might be formed through the transition state **B-TS3_S** (-39.0 kcal/mol) and **B-TS3_R** (-36.4 kcal/mol) with subsequent regeneration of **Cat-Rh** through the substrate exchange, a process that is also exergonic (-53.6 kcal/mol). Comparison of the enantioselective transition states in pathway **A** reveals that the energy barrier of **A-TS3_S** is 3.5 kcal/mol lower than that of **B-TS3_S** in pathway **B**, implying that the formation of bromine product is less favorable. In addition, the **CP-Cs** catalysis mechanism was considered. The intermediate **A-IM3-iso**, in combination with imine and **CP-Cs**, generates the complex **A-IM4'** (-39.5 kcal/mol). However, the free energy of **A-IM4'** is 1.5 kcal/mol higher than that of **A-IM4**, indicating that the **CP-Cs** catalysis mechanism is less favored than the CPA mechanism in pathway **A**. In conclusion, these calculations indicate that the formation of the enantioselective *S*-product **5** is more competitive when catalyzed by the CPA mechanism.

To uncover the origin of enantioselectivity control, we performed an Independent Gradient Model based on Hirshfeld partition (IGMH) analysis to evaluate noncovalent interactions on the structures of **A-TS3_S** and **A-TS3_R**. As shown in the Fig. 8, several types interaction between the fragment **A** (CPA and $Rh_2(OAc)_4$) and fragment **B** (imine

and enol) were observed. Notably, there is a stronger C-H...O interaction exit in **A-TS3_S** compared to **A-TS3_R** (b). The C-H...O distance between the hydrogen atom of imine and the oxygen atom of $Rh_2(OAc)_4$ in **A-TS3_S** is shorter than that in **A-TS3_R** (**A-TS3_S**, 1.940 Å vs **A-TS3_R**, 2.003 Å) (b²), indicating a more significant C-H...O interaction in **A-TS3_S**. Moreover, the green isosurface (C-H... π interactions) between the phenanthrene of CPA and the fragment **B** in **A-TS3_S** is larger than that in **A-TS3_R** (c), indicating a stronger C-H... π interaction in **A-TS3_S**. Furthermore, dispersion interactions are observed not only between the H atom of imine and the methyl of $Rh_2(OAc)_4$ (e¹) but also between the benzene group of imine and the phenanthrene of CPA (e²). The isosurface of these interactions (e¹ and e²) are more pronounced in **A-TS3_S** than in **A-TS3_R**, further supporting the enantioselectivity. Taken together, these noncovalent interactions play a pivotal role in the enantioselectivity control, with a clear preference for the formation of the *S*-product in **A-TS3_S**.

Based on the insights from control reactions and previous studies^{27,30,58}, we proposed a plausible reaction mechanism, as illustrated in Fig. 9. The reaction begins with the decomposition of diazo compound **1** in the presence of a rhodium catalyst, forming a carbynoid intermediate **A**. This intermediate undergoes nucleophilic attack by diol **2**, resulting in the formation of ylide **B**. Ylide **B** subsequently transforms into a Fischer-type alkoxy-Rh-carbene **C** through the cleavage of the C-Br bond and the release of HBr. The newly formed

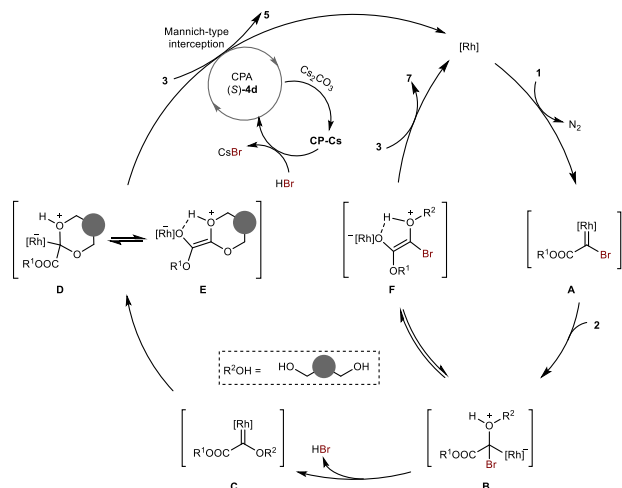


Fig. 9 | Reaction mechanism. Proposed reaction mechanism for chiral phosphoric acid-catalyzed asymmetric trifunctionalization involving α -halo Rh-carbenes.

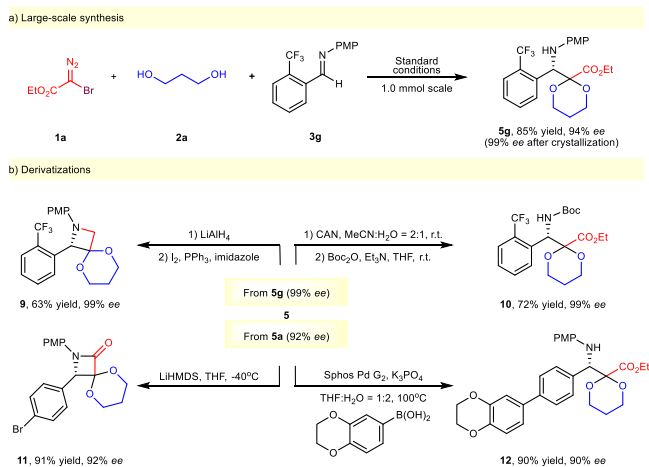


Fig. 10 | Synthetic applications. **a** Large scale synthesis of compound **5g**. **b** Derivative transformations of compound **5a** or **5g**.

carbene species **C** can then react intramolecularly with the alcohol, leading to the formation of cyclic ylide **D**, which exists in equilibrium with its enolate forms **E**. This active intermediate **E** is intercepted by chiral CPA **4** activated imine **3**, leading to the formation of Mannich-type products **5** and the regeneration of the catalysts. Simultaneously, CPA can be converted to **CP-Cs** in the presence of Cs_2CO_3 , and the **CP-Cs** salt can subsequently be acidified by the released **HBr** to regenerate CPA. Alternatively, byproduct **7** can be formed when electrophilic imines **3** react with enolate intermediate **F**, which is in equilibrium with ylide intermediate **B**.

Subsequently, we scaled up the reaction to a mmol scale, observing no adverse effect on the yield and stereoselectivity of product **5g**. After simple crystallization, the enantiomeric excess of the product was further improved to 99% (Fig. 10a). Next, we explored additional transformations of the readily produced β -amino esters using commercially available reagents (Fig. 10b). Reduction of the ester group to a hydroxyl group by LiAlH_4 , producing amino alcohol which underwent cyclization with I_2/PPh_3 , resulting in the formation of optically pure spiroazetidine **9** in 63% yield. Moreover, the PMP group on the nitrogen could be removed by treatment with ceric ammonium nitrate (CAN), generating the free amine, which was subsequently protected with Boc_2O under basic conditions, yielding compound **10** in a good 72% yield with 99% *ee*. Intramolecular amidation of compound **5a** using

LiHMDS yielded spiro lactam **11** in high 91% yield and with 92% *ee*. Notably, the Suzuki coupling reaction was also compatible with this skeleton, producing compound **12** in 90% yield with 90% *ee*. To highlight the synthetic value of this strategy, we evaluated the anti-proliferative activity of the chiral α -cyclic ketal β -amino esters using the CCK-8 assay in three human cancer cell lines: A549 (lung adenocarcinoma), HCT116 (colorectal cancer), and MIA-PaCa2 (pancreatic cancer). Preliminary results showed that most compounds displayed potent anti-proliferative activity across all tested cell lines (Table S1). Among these, the Pinanediol-derived compound **5bj** demonstrated exceptional potency, with IC_{50} values ranging from approximately 1 to 4 μM , outperforming Taxol in select cell lines (Fig. S6; see Supplementary Information for details).

In summary, we have developed an efficient chiral phosphoric acid-catalyzed asymmetric three-component reaction that employs α -halo Rh-carbenes as carbynoids in conjunction with diols and imines. This method facilitates the synthesis of a broad array of α -cyclic ketal β -amino esters with broad substrate scope, high yields, and excellent enantioselectivities under mild conditions. Mechanistic studies indicate that the reaction's success relies on the in situ formation of functionalized Fischer-type alkyloxy Rh-carbenes, with cesium carbonate playing a pivotal role in achieving precise enantioselective control. The origins of the high enantioselectivity have been further clarified through DFT calculations. Ongoing research in our laboratory is focused on expanding this reaction to higher-order multicomponent systems (four or more components) and exploring its potential applications in biological activity testing.

Methods

General procedure for the asymmetric trifunctionalization reaction

In a 10-mL oven-dried vial equipped with a magnetic stirring bar, **3** (0.10 mmol, 1.0 equiv.), **2** (0.30 mmol, 3.0 equiv.), Cs_2CO_3 (0.3 mmol, 3.0 equiv.), $\text{Rh}_2(\text{OAc})_4$ (2.0 mol%), CPA **4d** (5.0 mol%) and 4 Å MS (150 mg) were combined in CH_2Cl_2 (1.5 mL). The cooled solution of diazo compound **1** or **11** (0.30 mmol, 3.0 equiv.) in CH_2Cl_2 (1.5 mL) was added to this mixture via a syringe pump in 0.5 h under a nitrogen atmosphere at 0 °C, and the reaction was running for 4 h under these conditions. Upon complete consumption of the starting material (monitored by TLC), the crude reaction mixture was then concentrated under vacuum, and the product was purified by column chromatography on silica gel to give the corresponding products in good to high yields. The enantioselectivity was determined by chiral HPLC analysis.

Reporting summary

Further information on research design is available in the Nature Portfolio Reporting Summary linked to this article.

Data availability

The data that support the findings of this study are available within the paper and its Supplementary Information. The cartesian coordinates of the optimized structures in this study are provided in Source Data file. Source data are provided with this paper. All data are available from the corresponding author upon request. Crystallographic data for the structures reported in this article have been deposited at the Cambridge Crystallographic Data Centre, under deposition numbers CCDC2298129 (5n). Copies of the data can be obtained free of charge via <https://www.ccdc.cam.ac.uk/structures/>. Source data are provided with this paper.

References

1. Yao, M.-H., Dong, S.-L. & Xu, X.-F. Asymmetric carbene transformations for the construction of all-carbon quaternary centers. *Chem. Eur. J.* e202304299 (2024).

- He, Y. et al. Recent advances in transition-metal-catalyzed carbene insertion to C-H bonds. *Chem. Soc. Rev.* **51**, 2759–2852 (2022).
- Zhu, D., Chen, L.-F., Fan, H.-L., Yao, Q.-L. & Zhu, S.-F. Recent progress on donor and donor–donor carbenes. *Chem. Soc. Rev.* **49**, 908–950 (2020).
- Cheng, Q.-Q., Deng, Y.-M., Lankelma, M. & Doyle, M. P. Cycloaddition reactions of enoldiazo compounds. *Chem. Soc. Rev.* **46**, 5425–5443 (2017).
- Zhang, D. & Hu, W.-H. Asymmetric multicomponent reactions based on trapping of active intermediates. *Chem. Rec.* **17**, 739–753 (2017).
- Guo, X. & Hu, W.-H. Novel multicomponent reactions via trapping of protic onium ylides with electrophiles. *Acc. Chem. Res.* **46**, 2427–2440 (2013).
- Zhang, M., Xu, X. & Hu, W. Multi-Component Reaction via gem-Difunctionalization of Metal Carbene. Ed. Che, C.-M., Wang, J. & Doyle, M. P. Wiley-VCH GmbH, 325–369 (2022).
- John, S. E., Gulati, S. & Shankaraiah, N. Recent advances in multicomponent reactions and their mechanistic insights: a triennium review. *Org. Chem. Front.* **8**, 4237–4287 (2021).
- Müller, T. J. J. Multicomponent reactions III. *Beilstein J. Org. Chem.* **15**, 1974–1975 (2019).
- Wang, Q., Wang, D.-X., Wang, M.-X. & Zhu, J.-P. Still unconquered: enantioselective Passerini and Ugi multicomponent reactions. *Acc. Chem. Res.* **51**, 1290–1300 (2018).
- Levi, L. & Müller, T. J. J. Multicomponent syntheses of functional chromophores. *Chem. Soc. Rev.* **45**, 2825–2846 (2016).
- Zarganes-Tzitzikas, T., Chandgude, A. L. & Dömling, A. Multi-component reactions, union of MCRs and beyond. *Chem. Rec.* **15**, 981–996 (2015).
- Wender, P. A. & Miller, B. L. Synthesis at the molecular frontier. *Nature* **460**, 197–201 (2009).
- Wehlan, H., Oehme, J., Schäfer, A. & Rossen, K. Development of scalable conditions for the Ugi reaction-application to the synthesis of (R)-Lacosamide. *Org. Process Res. Dev.* **19**, 1980–1986 (2015).
- Liu, H.-X., William, S., Herdtweck, E., Botros, S. & Dömling, A. MCR synthesis of praziquantel derivatives. *Chem. Biol. Drug Des.* **79**, 470–477 (2012).
- Malaquin, S. et al. Ugi reaction for the synthesis of 4-aminopiperidine-4-carboxylic acid derivatives. Application to the synthesis of carfentanil and remifentanil. *Tetrahedron Lett.* **51**, 2983–2985 (2010).
- Znabet, A. et al. A highly efficient synthesis of telaprevir by strategic use of biocatalysis and multicomponent reactions. *Chem. Commun.* **46**, 7918–7920 (2010).
- Kalinski, C. et al. Multicomponent reactions as a powerful tool for generic drug synthesis. *Synthesis* **24**, 4007–4011 (2008).
- Wei, R., Wang, X.-F., Hu, C.-P. & Liu, L.-L. Synthesis and reactivity of copper carbyne anion complexes. *Nat. Synth.* **2**, 357–363 (2023).
- Rao, J.-H. et al. A triplet iron carbyne complex. *J. Am. Chem. Soc.* **145**, 25766–25775 (2023).
- Yang, Y.-H. & Wang, C.-Y. Forging three single bonds on one carbon via metal carbynes or carbyne equivalents. *Chin. J. Chem.* **39**, 3481–3484 (2021).
- Fürstner, A. Alkyne metathesis on the rise. *Angew. Chem. Int. Ed.* **52**, 2794–2819 (2013).
- Bogoslavsky, B. et al. Do carbyne radicals really exist in aqueous solution? *Angew. Chem. Int. Ed.* **51**, 90–94 (2011).
- Xue, W.-C. et al. Nickel-catalyzed formation of quaternary carbon centers using tertiary alkyl electrophiles. *Chem. Soc. Rev.* **50**, 4162–4184 (2021).
- Süsse, L. & Stoltz, B. M. Enantioselective formation of quaternary centers by allylic alkylation with first-row transition-metal catalysts. *Chem. Rev.* **121**, 4084–4099 (2021).
- Feng, J.-J., Holmes, M. & Krische, M. J. *Chem. Rev.* **117**, 12564–12580 (2017).
- Palomo, E. et al. Generating Fischer-type Rh-carbenes with Rh-carbynoids. *J. Am. Chem. Soc.* **145**, 4975–4981 (2023).
- Tu, H.-F., Jeandin, A. & Suero, M. G. Catalytic synthesis of cyclopropenium cations with Rh-carbynoids. *J. Am. Chem. Soc.* **144**, 16737–16743 (2022).
- Wang, Z.-F., Jiang, L.-Y., Sarró, P. & Suero, M. G. Catalytic cleavage of C(sp²)-(sp²) bonds with Rh-carbynoids. *J. Am. Chem. Soc.* **141**, 15509–15514 (2019).
- Qian, Y. et al. Enantioselective multifunctionalization with Rh-carbynoids. *J. Am. Chem. Soc.* **145**, 26403–26411 (2023).
- Zhao, W.-W. et al. Trifluoromethyl rhodium-carbynoid in [2+1+2] cycloadditions. *Angew. Chem. Int. Ed.* **63**, e202318887 (2024).
- Timmann, S., Wu, T.-H., Golz, C. & Alcarazo, M. Reactivity of α -diazo sulfonium salts: rhodium-catalysed ring expansion of indenones to naphthalenes. *Chem. Sci.* **15**, 5938–5943 (2024).
- Wang, X.-Y. et al. Convergent synthesis of 1,4-dicarbonyl Z-alkenes through three-component coupling of alkynes, α -diazo sulfonium triflate, and water. *J. Am. Chem. Soc.* **144**, 4952–4965 (2022).
- Dong, J.-Y. et al. Visible light-induced [3+2] cyclization reactions of hydrazones with hypervalent iodine diazo reagents for the synthesis of 1-amino-1,2,3-triazoles. *Adv. Synth. Catal.* **363**, 2133–2139 (2021).
- Li, X.-D., Golz, C. & Alcarazo, M. α -Diazo sulfonium triflates: synthesis, structure, and application to the synthesis of 1-(dialkylamino)-1,2,3-triazoles. *Angew. Chem. Int. Ed.* **60**, 6943–6948 (2021).
- Bonge, H. T., Pintea, B. & Hansen, T. Highly efficient formation of halodiazoacetates and their use in stereoselective synthesis of halocyclopropanes. *Org. Biomol. Chem.* **6**, 3670–3672 (2008).
- Bonge, H. T. & Hansen, T. Intermolecular C-H and Si-H Insertion Reactions with Halodiazoacetates. *Synthesis* **2009**, 91–96 (2008).
- Kaupang, Å. & Bonge-Hansen, T. α -Bromodiazoacetamides - a new class of diazo compounds for catalyst-free, ambient temperature intramolecular C-H insertion reactions. *Beilstein J. Org. Chem.* **9**, 1407–1413 (2013).
- Mortén, M., Hennem, M. & Bonge-Hansen, T. Synthesis of quinoline-3-carboxylates by a Rh(II)-catalyzed cyclopropanation-ring expansion reaction of indoles with halodiazoacetates. *Beilstein J. Org. Chem.* **11**, 1944–1949 (2015).
- Mortén, M., Hennem, M. & Bonge-Hansen, T. On the cause of low thermal stability of ethyl halodiazoacetates. *Beilstein J. Org. Chem.* **12**, 1590–1597 (2016).
- Peeters, S., Berntsen, L. N., Rongved, P. & Bonge-Hansen, T. Cyclopropanation–ring expansion of 3-chloroindoles with α -halodiazoacetates: novel synthesis of 4-quinolone-3-carboxylic acid and norfloxacin. *Beilstein J. Org. Chem.* **15**, 2156–2160 (2019).
- Schnaars, C., Hennem, M. & Bonge-Hansen, T. Nucleophilic halogenations of diazo compounds, a complementary principle for the synthesis of halodiazo compounds: experimental and theoretical studies. *J. Org. Chem.* **78**, 7488–7497 (2013).
- Wu, F.-P. et al. Ring expansion of indene by photoredox-enabled functionalized carbon-atom insertion. *Nat. Catal.* **7**, 242–251 (2024).
- Sicignano, M. & Costa, P. Drug design via single-carbon atom insertion. *Nat. Catal.* **7**, 224–226 (2024).
- Liu, S.-P. et al. Tunable molecular editing of indoles with fluoroalkyl carbenes. *Nat. Chem.* <https://doi.org/10.1038/s41557-024-01468-2> (2024).
- Tang, J. et al. Rhodium-catalyzed formal four-component reaction with hypervalent iodine diazoesters, alcohols, and isatins for the synthesis of multi-functionalized oxindoles. *Org. Chem. Front.* **11**, 1106–1111 (2024).
- Ma, C.-Q. et al. Synthesis and Characterization of Donor-Acceptor Iron Porphyrin Carbenes and Their Reactivities in N-H Insertion and Related Three-Component Reaction. *J. Am. Chem. Soc.* **145**, 4934–4939 (2023).

48. Dong, S.-L. et al. Construction of chiral quaternary carbon centers via asymmetric metal carbene *gem*-dialkylation. *Angew. Chem. Int. Ed.* **62**, e202302371 (2023).
49. Kang, Z.-H. et al. Ternary catalysis enabled three-component asymmetric allylic alkylation as a concise track to chiral α,α -disubstituted ketones. *J. Am. Chem. Soc.* **143**, 20818–20827 (2021).
50. Kang, Z.-H. et al. Asymmetric counter-anion-directed amino-methylation: synthesis of chiral β -amino acids via trapping of an enol intermediate. *J. Am. Chem. Soc.* **141**, 1473–1478 (2019).
51. Ozawa, M. et al. Contribution of cage-shaped structure of physalins to their mode of action in inhibition of NF- κ B activation. *ACS Med. Chem. Lett.* **4**, 730–735 (2013).
52. Hosoya, T., Arai, M. A., Koyano, T., Kowithayakorn, T. & Ishibashi, M. Naturally occurring small-molecule inhibitors of Hedgehog/GLI-mediated transcription. *ChemBioChem* **9**, 1082–1092 (2008).
53. Krojer, M., Müller, C. & Bracher, F. Steroidomimetic amino-methyl spiroacetals as novel inhibitors of the enzyme Δ 8,7-sterol isomerase in cholesterol biosynthesis. *Arch. Pharm.* **347**, 108–122 (2014).
54. Franchini, S. et al. 1,3-Dioxane as a scaffold for potent and selective 5-HT_{1A}R agonist with in-vivo anxiolytic, anti-depressant and anti-nociceptive activity. *Eur. J. Med. Chem.* **176**, 310–325 (2019).
55. Menikarachchi, L. C. & Gascon, J. A. QM/MM approaches in medicinal chemistry research. *Curr. Top. Med. Chem.* **10**, 46–54 (2010).
56. Dapprich, S., Komáromi, I., Byun, K. S., Morokuma, K. & Frisch, M. J. A new ONIOM implementation in Gaussian98. Part I. The calculation of energies, gradients, vibrational frequencies and electric field derivatives. *J. Mol. Struct.: Theochem.* **461–462**, 1–21 (1999).
57. Senn, H. M. & Thiel, W. QM/MM methods for biomolecular systems. *Angew. Chem. Int. Ed.* **48**, 1198–1229 (2009).
58. Li, L. et al. A carbene relay strategy for cascade insertion reactions. *Angew. Chem. Int. Ed.* **62**, e202312793 (2023).

Acknowledgements

Support for this research from the National Natural Science Foundation of China (92256301 W.H., 92056201 W.H.), the National Key Research and Development Program of China (2023YFC3404500 Y.Q.), Guangdong Provincial Key Laboratory of Chiral Molecule and Drug Discovery (2023B1212060022 W.H.), Natural Science Foundation of Guangdong Province (2023A1515011486 Y.Q.) and Key-Area Research and Development Program of Guangdong Province (2022B1111050003 Y.Q., 2022B1111070004 W.H.) are greatly acknowledged.

Author contributions

Y.Q. and W.H. designed the experiments and analyzed the data. X.Y. performed the experiments and analyzed the data. X.Z. performed the theoretical calculations. Y.Q. and W.H. wrote the manuscript. Y.Q. and W.H. conceived and supervised the project. All authors discussed the results and commented on the article.

Competing interests

The authors declare no competing interests.

Additional information

Supplementary information The online version contains supplementary material available at <https://doi.org/10.1038/s41467-025-56446-0>.

Correspondence and requests for materials should be addressed to Wenhao Hu or Yu Qian.

Peer review information *Nature Communications* thanks the anonymous reviewer(s) for their contribution to the peer review of this work. A peer review file is available.

Reprints and permissions information is available at <http://www.nature.com/reprints>

Publisher's note Springer Nature remains neutral with regard to jurisdictional claims in published maps and institutional affiliations.

Open Access This article is licensed under a Creative Commons Attribution-NonCommercial-NoDerivatives 4.0 International License, which permits any non-commercial use, sharing, distribution and reproduction in any medium or format, as long as you give appropriate credit to the original author(s) and the source, provide a link to the Creative Commons licence, and indicate if you modified the licensed material. You do not have permission under this licence to share adapted material derived from this article or parts of it. The images or other third party material in this article are included in the article's Creative Commons licence, unless indicated otherwise in a credit line to the material. If material is not included in the article's Creative Commons licence and your intended use is not permitted by statutory regulation or exceeds the permitted use, you will need to obtain permission directly from the copyright holder. To view a copy of this licence, visit <http://creativecommons.org/licenses/by-nc-nd/4.0/>.

© The Author(s) 2025